DOI: 10.1002/anie.201207813

Structure Elucidation

Evidence for Multicenter Bonding in Dianionic Tetracyanoethylene Dimers by Raman Spectroscopy[**]

Juan Casado, Paula Mayorga Burrezo, Francisco J. Ramírez, Juan T. López Navarrete,* Saul H. Lapidus, Peter W. Stephens,* Hoa-Lan Vo, Joel S. Miller,* Fernando Mota, and Juan J. Novoa**

Long, multicenter C—C bonds within dimers of neutral or charged radicals, for example, π-$[TCNE]_2^{2-}$ (TCNE = tetracyanoethylene, Figure 1) have been established from spectroscopic (UV/Vis/NIR, ESR, NMR and IR) studies, structural (crystallographic) evidence, and theoretical support.[1–8] $[TCNE]_2^{2-}$ is stable in the solid state as a consequence of the attractive cation$^+$···anion$^-$ interactions exceeding the repulsive cation$^+$···cation$^+$ and $[TCNE]^{\bullet-}$···$[TCNE]^{\bullet-}$ interactions, and is assisted by the dispersion and bonding energetic components acting between the two $[TCNE]^{\bullet-}$ fragments.[6,8] Thus, π-$[TCNE]_2^{2-}$ anion is diamagnetic, and has an observed closed-shell singlet ground state. Its long multicenter bond is best described as a two-electron/four-center ($2e^-/4c$) bond,[1,8] with an approximately 2.9 Å intradimer separation. To date there are approximately 25 $[TCNE]_2^{2-}$ structural determinations, and although the cations range from point charges with significant electrostatic interactions, for example, Tl^+,[9] to distant bulky cations, for example, $[Cr(C_6H_6)_2]^+$,[10] the $[TCNE]_2^{2-}$ dimer is essentially identical. In addition to the similar $[TCNE]_2^{2-}$ structures, the IR spectra are similar.

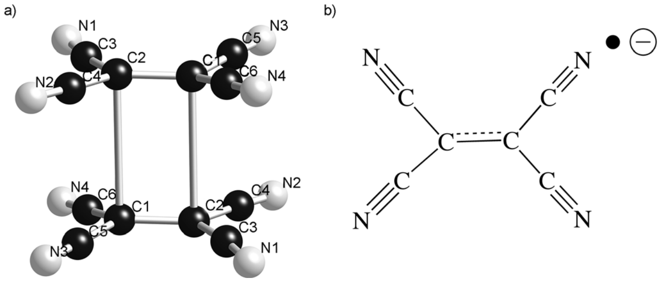

Figure 1. Structure of $[TCNE]_2^{2-}$ in $K_2[TCNE]_2$: C1—C2′ = 2.908(8); C1—C2 = 1.439(8) (a), and $[TCNE]^{\bullet-}$ (b). For $Rb_2[TCNE]_2$: C1—C2′ = 2.928(5); C1—C2 = 1.539(5) Å.

The experimental information on the long, multicenter bond in π-$[TCNE]_2^{2-}$, as with the other radical ion or neutral dimers, still lacks of direct evidence on its strength. Previous experimental studies provided estimates of its strength in solvated dimers based on the enthalpy of formation from the thermodynamic equilibrium constant.[4]

Raman spectroscopic studies have the potential to provide a deeper insight into the properties of long bonds by exploring the shape of the intradimer C···C stretching vibrational mode. This mode is expected to be Raman-active based on symmetry considerations, and its observation unequivocally characterizes the presence of the long, multicenter bond in π-$[TCNE]_2^{2-}$.

Since the structure of π-$[TCNE]_2^{2-}$ is invariant to the nature of the cation, the K^+ salt in addition to being representative is far simpler to study computationally and interpret the vibrational data because of fewer IR and Raman modes, and was selected for our initial study. We have tested the validity of this idea by applying the same procedure to the Rb^+ and Cs^+ salts that also possess similar π-$[TCNE]_2^{2-}$ dimers.

From the vibrational spectrum of π-$[TCNE]_2^{2-}$ in a $K_2[TCNE]_2$ crystal, the force constants associated with the

---

[*] Prof. J. Casado, P. M. Burrezo, Prof. F. J. Ramírez,
Prof. J. T. L. Navarrete
Departamento de Química Física, Universidad de Málaga
29071 Málaga (Spain)
E-mail: casado@uma.es
teodomiro@uma.es

Dr. S. H. Lapidus, Prof. P. W. Stephens
Department of Physics and Astronomy, Stony Brook University
Stony Brook, NY 11794 (USA)
E-mail: Peter.Stephens@sunysb.edu

H.-L. Vo, Prof. J. S. Miller
Department of Chemsitry, University of Utah
Salt Lake City, UT 84112-0850 (USA)
E-mail: jsmiller@chem.utah.edu

Prof. F. Mota, Prof. J. J. Novoa
Departamento de Química Física & IQTCUB
Facultad de Química, Universidad de Barcelona
Av. Diagonal, 647, 08028 Barcelona (Spain)
E-mail: juan.novoa@ub.edu

[**] The Malaga team thanks the MINECO for funding (project numbers CTQ201233733 and P06FQM-4708). J.S.M and H.-L.V. appreciate the continued support by the U. S. Department of Energy Division of Material Science (grant number DE-FG03-93ER45504) for chemical synthesis, spectroscopic and magnetic studies. F.M. and J.J.N. thank the MINECO for funding (grant number MAT2011-25972), and the Catalan Autonomous Government (grant number 2009 SGR 1203). They also thank for the allocation of computer time done by CESCA and BSC. Use of the National Synchrotron Light Source, Brookhaven National Laboratory for powder diffraction studies (S.H.L. and P.W.S) was supported by the U.S. Department of Energy, Office of Basic Energy Sciences, under contract number DE-AC02-98CH10886.

Supporting information for this article is available on the WWW under http://dx.doi.org/10.1002/anie.201207813.

intradimer C···C stretching mode can be accurately determined. This permits the estimation of the strength of the multicenter C–C bonds in its ionic crystals within the context of Badger's empirical relationship between stretching force constant and strength.[11] Details are given in the Supporting Information.

Herein, we report a combined theoretical/experimental study of the Raman vibrational spectra of $K_2[TCNE]_2$, identification of the elusive intradimer C···C stretching mode, and determination of the corresponding force constant using the same programs and procedure reported for π-dimers of oligothiophene radical cations.[12] This is described in detail in the Supporting Information.

$A_2[TCNE]_2$ was prepared from the reaction of AI (A = K, Rb, Cs) and TCNE in MeCN,[13] and the structures for A = K and Rb were determined from high-resolution X-ray powder diffraction data[14] obtained at beamline X16C of the National Synchrotron Light Source located at Brookhaven National Laboratory. $A_2[TCNE]_2$ is isostructural to $Tl_2[TCNE]_2$.[9] and posses π-$[TCNE]_2^{2-}$ dimers with intradimer C–C separations of 2.908(8) Å (Figure 1 a) and 2.928(5) Å, respectively. The structure of $Cs_2[TCNE]_2$ was previously reported and has a 2.887(6) Å intradimer separation.[15]

The 1064 nm Raman spectrum of $K_2[TCNE]_2$ is shown in the top of Figure 2.[16] Independently, the theoretical UM06L/aug-cc-pVTZ[17] Raman spectrum was computed (Figure 2 bottom). These two spectra have a similar intensity pattern with a small mean deviation of 30.1 cm^{-1} between the experimental and theoretical frequencies; thus, the calculated force field (potential-energy surface) for $K_2[TCNE]_2$ is very reliable.

A normal mode analysis (see the Supporting Information and Refs. [7] and [10] therein) was done on $K_2[TCNE]_2$ by defining a full space of vibrational locally symmetrized internal coordinates that includes the motions of the K^+ cations relative to the $[TCNE]^-$. The new internal coordinate force field, which fully reproduces the theoretical Raman spectrum provided by the Cartesian coordinate force field from the ab initio calculation, allows for a quantitative description and assignment of the vibrational Raman spectrum in terms of physically meaningful coordinates. The far-infrared 100–300 cm^{-1} region of the Raman spectrum is particularly relevant since the π-$[TCNE]_2^{2-}$ interfragment vibrations are expected in this range. The normal mode analysis allows us to evaluate the weight of the C···C internal coordinate in the vibrational bands and to determine the force constant and strength of the interfragment bond.

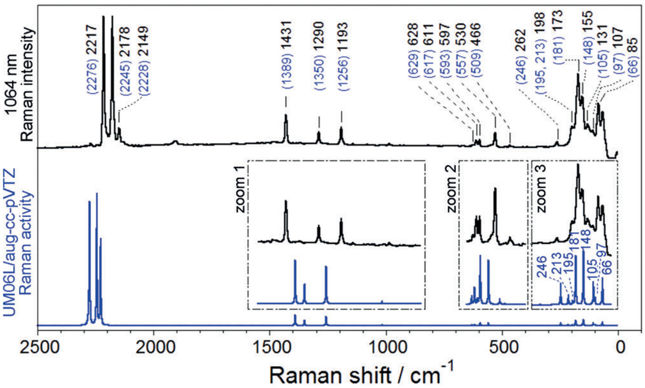

Figure 2. Top) Room-temperature solid-state 1064 nm FT-Raman spectrum of $K_2[TCNE]_2$. Bottom) UM06L/aug-cc-pVTZ Raman spectrum of $K_2[TCNE]_2$. The insets show the specific spectral regions. The experimental peak positions are in black, and the computed values are in blue and in parenthesis.

The nature of the most intense Raman bands for $K_2[TCNE]_2$ (Figure 2) in terms of vibrational internal coordinates is summarized in Table 1 while the key modes are shown in Figure 3 (a full description of all bands and the vibrational modes are collected in Tables S1–S3 and Figures S2–S6).

The modes above 2000 cm^{-1} are the symmetric and antisymmetric combinations of the intrafragment ν(C≡N) stretches. Those in the 1500–1000 cm^{-1} region are the symmetric and antisymmetric combinations of the central ν(C–C) stretches or δ(CCC) bendings that were assigned from their counterparts in the IR spectrum and computed for the $K_2[TCNE]_2$ aggregate (Figure S7 bottom). The 1431 cm^{-1} band (theory: 1389 cm^{-1}) is the symmetric combination of the central ν(C–C) stretches from each $[TCNE]^-$ unit (the

Table 1: Assignment of the main Raman bands for $K_2[TCNE]_2$, the main internal coordinates of which are due to motions within the $[TCNE]_2^{2-}$ dimer [the theoretical spectrum was computed at the UM06 L/aug-ccp-VTZ level; ν (stretching), δ (in-plane bending), γ (out-of-plane bending)]. Band intensities which exceeds 2 $Å^4$ amu^{-1} are listed and the complete computed set of Raman bands is given.

Mode	Exp.	Theo.	Potential-Energy Contribution
ν_1	2217	2280, 2276[a]	88 ν(C≡N), 12 ν(C–C)
ν_2	2178	2245	85 ν(C≡N), 15 ν(C–C)
ν_3	2149	2228	85 ν(C≡N), 15 ν(C-C)
ν_4	1431	1389	78 ν(C=C), 22 ν(C–C)
ν_5	1290	1350	66 ν(C–C), 34 δ(C···C–C)
ν_6	1193	1256	90 ν(C–C), 10 δ(C···C–C)
ν_7	628	629	52 γ(C–C≡N), 34 δ(C···C–C), 14 δ(cycle)
ν_8	611	617	36 δ(C–C≡N), 35 δ(C–C–C), 19 ν(C–C), 10 δ(C···C–C)
ν_9	597	593	52 ν(C–C), 31 ν(C=C), 17 δ(C–C≡N)
ν_{10}	530	557	64 γ(C–C≡N), 36 δ(C···C–C)
ν_{12}	466	509	78 δ(C–C≡N), 22 δ(C···C–C)
ν_{13}	262	246	55 δ(C–C≡N), 45 δ(C···C–C)
ν_{14}	198	213, 195	35 ν(K^+–N), 19 δ(C···C-C), 17 δ(C–C–C), 14 ν(C···C)
ν_{15}	173	181	61 ν(C···C), 39 δ(C···C–C)
ν_{16}	155	148	82 ν(C···C), 18 δ(C–C–C)
ν_{17}	131	105	55 δ(C···C–C), 23 δ(cycle), 22 ν(K^+–N)
ν_{18}	107	97	44 δ(C–C–C), 26 δ(C–C≡N), 15 ν(C···C), 15 δ(C···C–C)
ν_{19}	85	66	100 δ(C···C–C)

[a] It is impossible to uniquely assign the observed dispersion, as two theoretical bands are close enough to form a single observed band, or become a shoulder of a band.

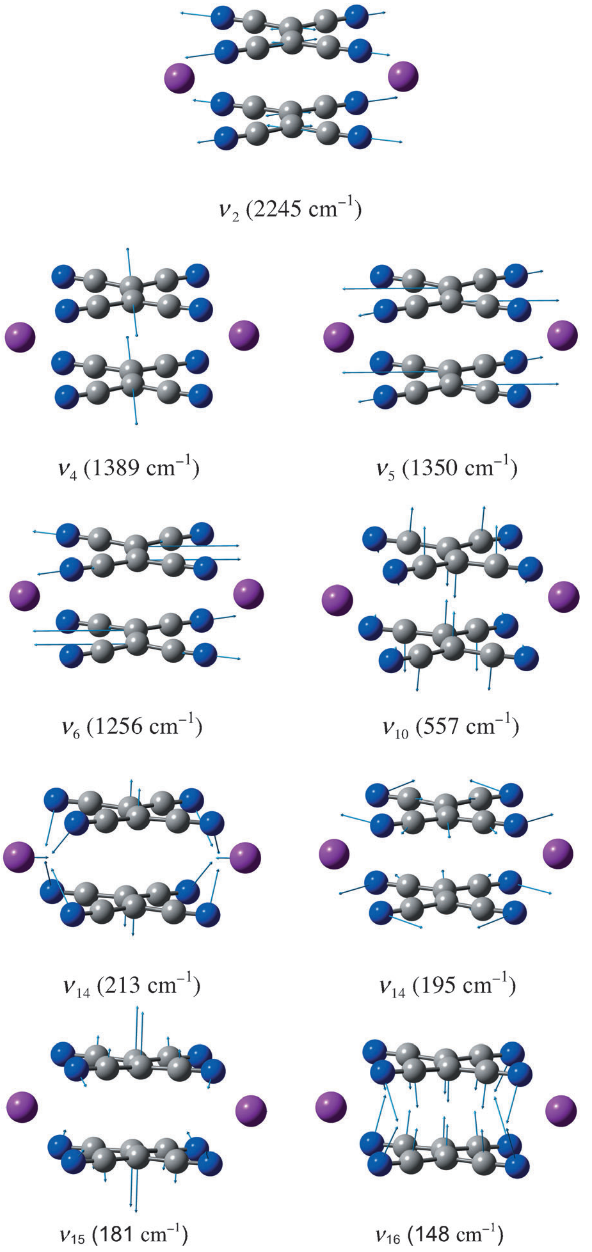

Figure 3. Vibrational normal modes associated with the most relevant Raman bands of the computed M06L/aug-cc-pVTZ theoretical Raman spectrum of $K_2[TCNE]_2$ (K is pink, N is blue, C is gray). The computed UM06L/aug-cc-p-VTZ frequency is also indicated.

antisymmetric combination vibration is not Raman active, but is observed in the IR spectrum[1,2]). The 1193 cm^{-1} (theory: 1256 cm^{-1}) dispersion has no Raman-active counterpart, and it is mostly associated to the antisymmetric combination mode of the central ν(C–C) stretch (with about 90% of the ν(C–C) contribution for each $[TCNE]^-$ unit). The other two bands are combinations of C(central)–C(lateral) stretches and C–C–C bending vibrations in each $[TCNE]^-$ unit.

Finally, below 550 cm^{-1}, the interfragment C···C stretches appear, initially with residual contributions of bending vibrations (above 300 cm^{-1}). UM06L-level vibrational calculations[18] indicate that only two of the experimental bands can be assigned to modes, the main contribution of which comes from the intradimer C···C stretching. These occur at 173 and 155 cm^{-1} (theory: 181 and 148 cm^{-1}) and are the only ones dominated by the ν(C···C) stretching. These Raman dispersions provide direct evidence for the existence of a long, multicenter bond between the two $[TCNE]^-$ fragments of π-$[TCNE]_2^{2-}$, and direct information for the shape of the potential energy curve for the $[TCNE]^{\bullet-}$···$[TCNE]^{\bullet-}$ interaction.

The validity of the π-$[TCNE]_2^{2-}$ vibrational assignments can be confirmed by comparing the Raman spectrum of $K_2[TCNE]_2$ with that for $[NBu_4]^+[TCNE]^{\bullet-}$ that only has isolated $[TCNE]^{\bullet-}$ units (Figure 4, the computational simulation of an isolated $[TCNE]^{\bullet-}$ is shown in Figures S6, and S7 and Table S3 on an UM06L geometry-optimized idealized K[TCNE] complex) that does not have dimers. The two spectra are distinctly different. In the 2200 cm^{-1} region the strongest band at 2195 cm^{-1} splits into two, with similar shifts towards higher (+22 cm^{-1}, 2195→2217 cm^{-1}) and lower (−18 cm^{-1}, 2195→2178 cm^{-1}) wavenumbers. This is due to vibrational couplings that result in the formation of symmetric and antisymmetric combinations. A similar splitting occurs in the 1300 cm^{-1} region. The computed Raman spectra of $K_2[TCNE]_2$ shows three medium intensity bands at 1256, 1350, and 1389 cm^{-1} that become two in $[NBu_4][TCNE]$. The Raman scattering at 1254 and 1193 cm^{-1} (Table S3, and Figures S6–S7) for $K_2[TCNE]_2$ correlate with the band at 1233 cm^{-1} for $[NBu_4][TCNE]$, which has a Raman intensity of zero and thus disappears. As indicated, the computed Raman spectrum of $K_2[TCNE]_2$ helps to identify the nature of these three bands (Table S3; Figures S6–S7). Finally, the most relevant differences between the Raman spectra of $K_2[TCNE]_2$ and $[NBu_4][TCNE]$ are in the far-IR region, that is, below 300 cm^{-1} (Figure 4b). In this region, which has not been explored before in other published studies, the $K_2[TCNE]_2$ Raman spectrum shows seven bands (ν_{13}–ν_{19} in Table 1). They differ from the $[NBu_4][TCNE]$ Raman spec-

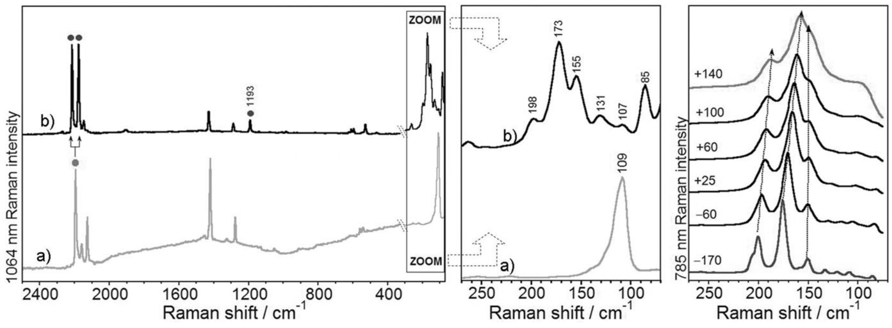

Figure 4. Left: room-temperature solid-state 1064 FT-Raman spectra of a) $[NBu_4][TCNE]$, and b) $K_2[TCNE]_2$. Center: Blow-up of the low wavelength region at room-temperature. Right: 785 nm low wavelength region Raman spectra[19] of $K_2[TCNE]_2$ as a function of the temperature.

trum, which has only one intense band at 109 cm^{-1} (associated to the synchronous in-plane bending vibration of the four CN groups combined with a NC stretching) that occurs at 131 cm^{-1} for K$_2$[TCNE]$_2$. However, the most relevant bands are at 173 and 155 cm^{-1} (ν_{15} and ν_{16}, the computed counterparts of which are located at 181 and 148 cm^{-1}, respectively). Furthermore, because their character is dominated by the interfragment C···C stretching, the computed C···C stretching force constant provides information on the curvature (around the equilibrium position) of the potential-energy curve, the reaction coordinate of which is defined by the elongation of this interfragment bond.

The temperature dependence of the low-frequency bands in the K$_2$[TCNE]$_2$ Raman spectra was also investigated to gain information about the stability of the long bond with temperature. Between −170 and +140 °C the 198 and 173 cm^{-1} bands (ν_{14} and ν_{15} in Table 1) move significantly to lower wavenumbers [Figure 4 (right)] with heating because of the strong anharmonicity of this vibrational mode. It was observed that 1) the stronger band at 173 cm^{-1} has the larger shift of −18 cm^{-1}, which is consistent with its 100 % contribution by vibrational modes involving the weak C···C bonds (Tables 1), and 2) the 198 cm^{-1} band moves −10 cm^{-1}. This later shift is additionally due to the relevant contribution of the K$^+$···N stretching that has the smaller molecular force constant (0.21 mdyn Å^{-1} in Table S3) as computed at the UM06L/aug-ccp-VTZ level.

The normal mode analysis provides harmonic force constants for the 13 locally symmetrized internal coordinates defined for K$_2$[TCNE]$_2$ (Tables S4–S6). By taking the stretching mode for a bond as internal coordinate, the bond strength can be quantitatively evaluated (such a force constant is now independent of the molecular vibrational normal mode used for its computation). For π-[TCNE]$_2^{2-}$ in K$_2$[TCNE]$_2$ the ν(C···C) stretching harmonic force constant is 0.45 mdyn Å^{-1} (using the UM06L/aug-ccp-VTZ second derivatives).

When the same procedure was applied to the Rb$^+$ analog, the ν(C···C) experimental Raman spectrum is theoretically simulated[20] with a ν(C···C) stretching harmonic force constant of 0.44 mdyn Å^{-1} in agreement with K$_2$[TCNE]$_2$. In addition, the Cs$^+$ analog was computed to have a stretching harmonic force constant of 0.45 mdyn Å^{-1}. This suggests the general validity for any π-[TCNE]$_2^{2-}$ dimer.

Typical force constants for the stretching modes of conventional covalent CC bonds are one order of magnitude higher, and are 19, 7, and 5 mdyn Å^{-1} for triple [ν(C≡C)], double [ν(C=C)], and single [ν(C−C)] bonds, respectively.[21] The average stretching force constant of a 3c hydrogen bond is about 0.20 mdyn Å^{-1}.[22] Thus, the long, 2e$^-$/4c C−C bond in K$_2$[TCNE]$_2$ has a stretching force constant higher than that reported for some hydrogen bonds.

Force constants can be quantitatively associated with bond energies in diatomic molecules.[11,23] However, due to geometrical and electronic structure relaxation, such correlation only holds qualitatively on polyatomic molecules.[24] The same qualitative linear correlation between force constant and interaction energy has been shown to exist for 47 hydrogen bonds with a correlation factor of 0.901.[25] Extrapolating this correlation, that is, $E_{\text{int}} = 1.011 + 32.386\, f$ (E_{int} in kcal mol^{-1} and f in mdyn Å^{-1}), for the long 2e$^-$/4c C−C bond has a bond energy of about 15 kcal mol^{-1} for the K$_2$[TCNE]$_2$. This estimate[26] is twice the experimental estimates from solution studies,[4] and from computational evaluations for related 2e$^-$/4c C−C [TCNE]$_2^{2-}$ bonds.[2]

In summary, the analysis of the Raman spectrum of K$_2$[TCNE]$_2$ in terms of internal coordinates and vibrational normal modes has enabled the determination of the stretching force constant, 0.45 mdyn Å^{-1}. From the aforementioned correlation between stretching force constants and interaction energy, the strength of the long bond in K$_2$[TCNE]$_2$ is estimated to be about 15 kcal mol^{-1}. Hence, the long, multicenter intradimer bond in the π-[TCNE]$_2^{2-}$ dimer is stronger than most van der Waals bonds present in molecular solids, and even stronger than some hydrogen bonds.

Received: September 27, 2012
Revised: March 4, 2013

Keywords: multicenter bonding · Raman spectroscopy · Rietveld analysis · structure elucidation

---

[1] J. J. Novoa, P. Lafuente, R. E. Del Sesto, J. S. Miller, *Angew. Chem.* **2001**, *113*, 2608; *Angew. Chem. Int. Ed.* **2001**, *40*, 2540.
[2] R. E. Del Sesto, J. S. Miller, P. Lafuente, J. J. Novoa, *Chem. Eur. J.* **2002**, *8*, 4894.
[3] J. J. Novoa, P. Lafuente, R. E. Del Sesto, J. S. Miller, *CrystEngComm* **2002**, *4*, 373.
[4] J.-M. Lu, S. V. Rosokha, J. K. Kochi, *J. Am. Chem. Soc.* **2003**, *125*, 12161.
[5] J. Jakowski, J. Simons, *J. Am. Chem. Soc.* **2003**, *125*, 16089.
[6] Y. Jung, M. Head-Gordon, *Phys. Chem. Chem. Phys.* **2004**, *6*, 2008.
[7] J. S. Miller, J. J. Novoa, *Acc. Chem. Res.* **2007**, *40*, 189.
[8] I. Garcia-Yoldi, J. S. Miller, J. J. Novoa, *J. Phys. Chem. A* **2007**, *111*, 8020.
[9] M. J. Johnson, C. Campana, B. M. Foxman, W. Desmarais, M. J. Vela, J. S. Miller, *Chem. Eur. J.* **2000**, *6*, 1805.
[10] J. S. Miller, D. M. O'Hare, A. Charkraborty, A. J. Epstein, *J. Am. Chem. Soc.* **1989**, *111*, 7853.
[11] R. M. Badger, *J. Chem. Phys.* **1934**, *2*, 128.
[12] J. Casado, K. Takimiya, T. Otsubo, F. J. Ramírez, J. J. Quirante, R. P. Ortiz, S. R. González, M. M. Oliva, J. T. Navarrete, *J. Am. Chem. Soc.* **2008**, *130*, 14028.
[13] In a glovebox (<1 ppm O$_2$), TCNE (250 mg, 1.95 mmol) was dissolved in 4 mL of acetonitrile. This solution was then added to a slurry of KCN (127 mg, 1.95 mmol) in 4 mL of acetonitrile. Upon addition, the solution quickly turned a dark green and was allowed to stir for 30 minutes at room temperature, after which it was placed in the freezer overnight. The dark green product was filtered and collected (yield 267 mg; 80 %). IR (KBr): $\tilde{\nu}$ = νCN 2201 (s), 2186 (sh), 2181 (s), 2172 (s); νCC 1368 cm (s); 1185 (w); δCCN 549 (w), 535 (w), 521 cm^{-1} (w). The Rb$^+$ and Cs$^+$ analogs were made by the same method.
[14] K$_2$[TCNE]$_2$: *C*2/*c*, $a = 12.9421(4)$, $b = 7.5763(2)$, $c = 15.0804(4)$ Å, $\beta = 96.540(3)°$, $V = 1469.06(8)$ Å^3, MW = 171.20 g mol^{-1}, $Z = 8$, $T = 295$ K; $R_{\text{wp}} = 4.13$ %; $R_{\text{exp}} = 3.01$ %. CCDC 892969 contains the supplementary crystallographic data for this article. These data can be obtained free of charge from The Cambridge Crystallographic Data Centre via www.ccdc.cam.ac.uk/data_request/cif. Rb$_2$[TCNE]$_2$: *C*2/*c*, $a = 13.2272(4)$, $b = 7.7058(2)$, $c = 15.4572(5)$ Å, $\beta = 96.316(3)°$, $V =$

1565.94(8) Å^3, MW = 213.57 g mol^{-1}, $Z = 8$, $T = 295$ K; $R_{wp} =$ 6.10%; $R_{exp} = 4.22$%. CCDC 918575 contains the supplementary crystallographic data for this article. These data can be obtained free of charge from The Cambridge Crystallographic Data Centre via www.ccdc.cam.ac.uk/data_request/cif.

[15] H. Bock, K. Ruppert, *Inorg. Chem.* **1992**, *31*, 5094.

[16] The 1064 nm excitation did not produce an observable fluorescence, and gave good resolution over the range of frequencies studied.

[17] Y. Zhao, D. G. Truhlar, *J. Chem. Phys.* **2006**, *125*, 194101; T. H. Dunning, Jr., *J. Chem. Phys.* **1989**, *90*, 1007.

[18] M. J. Frisch et al., Gaussian 09, Revision A.1, Gaussian, Inc., Wallingford CT, **2009**.

[19] Due to technical reasons for variable temperature measurements in the far-IR region, the best resolution is obtained with a 785 nm laser.

[20] Note that the experimental and computed spectra of Rb_2[TCNE]$_2$ and K_2[TCNE]$_2$ are quite similar. Furthermore, the computed binding energy of Rb_2[TCNE]$_2$ is similar to that of K_2[TCNE]$_2$, Cs_2[TCNE]$_2$, and [TTF]$_2$[TCNE]$_2$ (I. Garcia-Yoldi, J. S. Miller, J. J. Novoa, *J. Phys. Chem. A* **2009**, *113*, 484). Thus, the cation does not affect the properties of the π-[TCNE]$_2^{2-}$ moiety.

[21] E. B. Wilson, J. C. Decius, P. C. Cross in *Molecular Vibrations: The Theory of Infrared and Raman Vibrational Spectra*, Dover Publications Inc., New York, **1955**, chap 8, p. 175.

[22] M. C. Shivaglal, S. Singh, *Int. J. Quantum Chem.* **1989**, *36*, 105; S. Singh, E. Knozinger, *Spectrochim. Acta Part A* **1992**, *48*, 1767.

[23] D. Cremer, E. Kraka, *Curr. Org. Chem.* **2010**, *14*, 1524.

[24] E. Kraka, D. Cremer, *ChemPhysChem* **2009**, *10*, 686.

[25] M. Freindorf, E. Kraka, E. Cremer, *Int. J. Quantum Chem.* **2012**, *112*, 3174.

[26] The correlation between a force constant and its interaction energy has been derived for several H-bonds, and is applied to long-distance bonds. However, in the absence of a large number of correlations for this kind of bonds the error bars of such approximation are unknown, but will be the subject of later systematic studies.